Atmos. Chem. Phys. Discuss., 13, C11218–C11231, 2014
www.atmos-chem-phys-discuss.net/13/C11218/2014/

Atmospheric Chemistry and Physics Discussions

Interactive comment on "Aqueous-phase photochemical oxidation and direct photolysis of vanillin – a model compound of methoxy-phenols from biomass burning" *by* Y. J. Li et al.

Y. J. Li et al.

lakeli@ust.hk

Received and published: 18 January 2014

We thank Prof. Collett for the comments to help improve the manuscript. Below we address those comments point-by-point. Our responses are denoted by "R". The original text to be changed is denoted by "O" and the changed text is denoted by "M".

Reviewer #2

Li et al. report very interesting results concerning the aqueous phase oxidation of vanillin, an important biomass burning emission. Oxidation by UV and by OH are both tested and the generation of secondary organic aerosol (SOA) mass and its com-

position examined. The experiments are well designed and the data analysis is robust and insightful. The findings are highly relevant to ACP readers and fill a current gap in knowledge concerning aqueous SOA formation from cloud processing of prescribed and wild fire emissions. I commend the authors on this impressive piece of work and have only a few suggestions and comments to improve a final version of the manuscript.

The authors use UPLC/ESI-TOFMS to report the composition of some product species. More information is needed regarding how the authors went from the elemental formulae provided by the TOFMS to the structures they present. Mention is made of fragmentation loss, but the analytical description provided in the supplement does not address the fragmentation approach used. I assume in-source fragmentation was employed, but this should be explicitly stated and relevant details provided.

R: Yes, the fragmentation was in-source fragmentation without pre-selecting a particular ion for fragmentation. Collision energy of -10.0 eV was set to perform the in-source collision induced dissociation. Those details of the ToF-MS operation are now included into Sect. 5.2 in the Supplementary Information as below.

M: The capillary voltage was 4000 V, with an end plate offset of -500 V. The nebulizer pressure was 3.0 bar and the dry gas was at 4.0 L/min with dry heater operating at 220 °C. In-source collision induced dissociation, with a collision energy of -10.0 eV, was used to generate some fragments for structural elucidation.

R: In addition to the last entry in Table S3, where proposed fragmentation losses leading to the observed fragment peaks are listed, a paragraph of structural elucidation is added in Sect. 5.2 in the Supplementary Information, as below.

M: Fragmentation information induced by in-source collision was used for structural elucidation. For example, we observed three peaks in the chromatogram (Figure S11) with m/z 167 $\pm$ 0.5 Da ([M – H]-). The mass spectra of these three peaks are shown in Figure S12 (panel a-c). The spectrum in Figure S12-b has a loss of CO2 (see also

Table S3), a characteristic loss of carboxylic acids (Li et al., 2011). This product is therefore believed to be a carboxylic acid, formed by oxidation in the carbonyl group of VL. The other two isobaric products do not have this CO2 loss (Figures S11-a and -c, and Table S3), thus they are believed to be formed with one oxygen atom added to the aromatic ring as OH group. The positions of the OH group in these two products are not known at this point. Likewise, two isobaric products with a molecular weight of 184 ([M-H]- = 183) are believed to be formed by adding one more oxygen atom to the above products. One of them (B184_a, Figure S12-d) is believed to be a carboxylic acid with one more OH group than B168_b, while the other has two OH groups added to the aromatic ring (Figure S11-e). The product B302_a is believed to be a dimer of VL by radical polymerization based on two reasons. First, the molecular formula (C16H14O6) is double of that of VL (C8H8O3) with two hydrogen atoms less, supporting a radical polymerization process (Sun et al., 2010). Second, the loss of two CH3 groups (Table S3) suggests that there are two building blocks with VL structure that bears two OCH3 groups contributing to the CH3 losses. There is little information of other dimers for structural elucidation and their structures are not proposed.

On a related note, is there a reason the authors did not scan below m/z 50 in the ESI-TOFMS analyses to look for the presence of smaller product molecules?

R: If the scan range was set to below m/z 50, ions from the solvent (H2O and MeOH) adducts would be detected and their abundance would be very high and might dominate the mass spectra. We want to avoid this for two reasons. First, as we used elution program in the LC part, the ratio between H2O and MeOH changed during an LC run. This would give a drifting background as relative abundance of the adduct ions would change according to the H2O/MeOH ratio. Second, too high intensities of solvent adduct ions almost continuously getting into the detector would probably shorten the lifetime of the detector.

Furthermore, scanning from m/z 50 does not provide any advantage in providing evidence of fragments of the [M – H]Âň- of oxalic acid (C2HO4+, m/z = 89), while deriva-

tization GC-MS clearly has confirmed the presence of oxalic acid. As mentioned in the main text (Section 3.4), the two major reasons of low sensitivity of LC-MS in detecting small oxygenates are 1) poor separation of those small oxygenates in reversed phase LC and 2) inefficient ionization in ESI for those very hydrophilic organics.

Please mention the volume of solution used for the reactor experiments.

R: information about the solution volume (300 mL) is now included in Sect. 2.1, as below.

O: An aqueous solution of. . .

M: A volume of 300 mL aqueous solution of. . .

The authors conclude in section 3.6 that vanillin loss through aqueous oxidation by UV light can be as important as vanillin oxidation in the gas phase. This claim needs to be better justified. In particular, I question whether the UV exposure (both wavelengths and intensity) utilized in the lab experiments is comparable to atmospheric conditions. If it is not comparable, the authors should explain how they scaled their aqueous results for comparison to atmospheric gas phase oxidation rates. They did a good job of this for vanillin's aqueous oxidation by OH but did not address it for the UV exposures.

R: This section is modified in the Supporting Information to provide the justification.
O: This decay rate is at least comparable to the gas-phase loss rate (1E-4 s-1) for VL, assuming a gas-phase oxidation rate constant of 10E-11 cm3 molecules-1 s-1 (Coeur-Tourneur et al., 2010) and a gas-phase OH concentration of 1E6 molecules cm-3 (Ervens et al., 2013). Therefore, even without H2O2 in the aqueous phase, the loss of methoxy-phenolic compounds like VL through the aqueous-phase process (with UV light) can be as important as that through gas-phase oxidation.

M: This decay rate is at least comparable to the gas-phase loss rate (1E-4 s-1) for VL, assuming a gas-phase oxidation rate constant of 10E-11 cm3 molecules-1 s-1 (Coeur-Tourneur et al., 2010) and a gas-phase OH concentration of 1E6 molecules

cm-3 (Ervens et al., 2013). Note that this decay rate was measured with a UV lamp of 254 nm, lower than wavelength with significant actinic flux in the troposphere (>290 nm). A simple calculation shows that with the absorption cross section of VL estimated from its molar absorption coefficient and an assumed quantum yield of 0.28 (resulting in the measured decay rate at 254 nm), the photolysis rate in the wavelength range of tropospheric importance (295-425 nm) is 7.06E-4 s-1. The details of the calculation are provided in Section 7 in the Supporting Information. Therefore, even without H2O2 in the aqueous phase, the loss of methoxy-phenolic compounds like VL through the aqueous-phase process (with UV light) can be as important as that through gas-phase oxidation.

R: A justification is provided in detail in the Supporting Information as Section 7.

M:

7. Estimation of photolysis rate in 295-425 nm

Wavelength-dependent photolysis rate (J) can be estimated from the absorption cross section ($\sigma(\lambda)$), the quantum yield (ÏŢ(λ)), and the solar actinic flux (I(λ)), all of which are wavelength dependent (Seinfeld and Pandis, 2006). The first two parameters, $\sigma(\lambda)$ and ÏŢ(λ), are also compound specific and are not readily available in the literature for VL. The last parameter, I(λ), can be estimated from the energy output of the UV lamp (UVP, Pen-ray 254 nm 9", model 97606-08) used in the experiments and from literature for typical tropospheric environments (Finlayson-Pitts and Pitts, 1986).

We first estimate JVL in our experiments under condition (B), assuming that the decay of VL under condition (B) was solely due to direct photolysis. Then we have (Seinfeld and Pandis, 2006):

d[VL]/dt=-k_decay×[VL]=-J_VL×[VL] J_VL=$\int \sigma$_VL (λ) ÏŢ_VL (λ)I(λ)dλ=$\sum \sigma$ ÌĚ_VL (λ) ÏŢ ÌĚ_VL (λ) I ÌĚ(λ)$\Delta\lambda$ãĂŮãĂŮ

where kdecay is our measured decay rate (s-1) under condition (B), JVL is the first-

order photolysis rate (s-1) of VL, σ_VL (λ) is the wavelength-dependent absorption cross section (cm2) of VL, ÏŢ_VL (λ) is the wavelength-dependent quantum yield of VL, and I(λ) is the solar actinic flux, or the photo flux from the UV lamp in our experiments. The integration is simplified by summing the photolysis rates in finite "bins" (with $\Delta\lambda$=5 nm), calculated from the average values of the required parameters (denoted by a bar over the symbols).

Absorption cross section can be estimated from molar absorption coefficient:

σ_VL (λ)=(ãĂŰ10ãĂŮˆ3×ε_VL (λ))/N_A

where ε_VL (λ) is the molar absorption coefficient (dm3/mol/cm) and N_A is the Avogadro constant (6.02E23 mol-1). Figure S14-a shows the molar absorption coefficient (from NIST) of VL from 220-350 nm in a red line (Talrose et al., 2007), and the calculated absorption cross section (σ_VL (λ), 290-425 nm, $\Delta\lambda$=5 nm) is shown as blue open symbols in Figure S14-a. The molar absorption coefficient beyond 350 nm, which is not included in NIST database, was assumed to decrease exponentially from 330 nm without major absorption band in this region for VL.

Absorption cross section for experiments under condition (B) is thus calculated.

σ ÌĚ_VL (254)=2.35×ãĂŰ10ãĂŮˆ(-20) ãĂŰcmãĂŮˆ2

The quantum yield during experiments under condition (B), ÏŢ ÌĚ_VL (254), is first assumed to be unity. Photon flux is calculated from the energy output (FUV, specified by the manufacturer) of the UV lamp, FUV = 5.4 mW/cm2 = 5.4E-3 J cm-2 s-1, at 0.75 inch (approximately half of the bottle radius), by:

I ÌĚ= F_UV/E_hv =F_UV/((h×c)/λ)=(5.4×ãĂŰ10ãĂŮˆ(-3) JãĂŰcmãĂŮˆ(-2) sˆ(-1))/((6.626×ãĂŰ10ãĂŮˆ(-34) J·s×2.998×ãĂŰ10ãĂŮˆ8 m sˆ(-1))/(254×ãĂŰ10ãĂŮˆ(-9) m))=6.92 × ãĂŰ10ãĂŮˆ15 photonsãĂŰ cmãĂŮˆ(-2) sˆ(-1)

Here Ehv is the energy of one photon, h is the Planck constant and c is the speed of light. The estimated JVL at 254 nm in our experiments is (assuming quantum yield of

1 photon-1 and wavelength width of 5 nm):

J_VL (254)=σ ÌĚ_VL (λ) ÏŢ ÌĚ_VL (λ) I ÌĚ(λ)$\Delta\lambda$=6.92 $\times$ ãĂŰ10ãĂŮˆ15 photonsãĂŰ cmãĂŮˆ(-2) sˆ(-1)$\times$2.35$\times$ãĂŰ10ãĂŮˆ(-20) ãĂŰcmãĂŮˆ2$\times$1$\times$5=8.13$\times$ãĂŰ10ãĂŮˆ(-4) sˆ(-1)

This estimated J_VL (254) is 3.5 times of the measured kdecay (2.3E-4 s-1) in our experiments under condition (B). We attribute this difference to the quantum yield of VL photolysis and hence assume a non-unity quantum yield for the whole wavelength:

ÏŢ ÌĚ_VL (λ)=(2.3 $\times$ ãĂŰ10ãĂŮˆ(-4))/(8.13 $\times$ ãĂŰ10ãĂŮˆ(-4))=0.28.

Using this quantum yield, we then estimate the photolysis rates of VL in the UV region of tropospheric importance (290-425 nm). The wavelength-dependent solar actinic flux in typical tropospheric environments (ground level, July 1, noon, 40°N, 298 K) is taken from (Finlayson-Pitts and Pitts, 1986) and is shown in red open symbols in Figure S14-b.The estimated photolysis rates are believed to be upper limits since wavelength-dependent quantum yields normally decrease, most likely exponentially, as wavelength increases.

Table S4 showed the estimated photolysis rates of VL in different wavelength “bins”. The photolysis rates of VL range from 10-5 to 10-4 s-1 for wavelength where VL has a strong absorption band, i.e., 300-350 nm. Beyond 350 nm, the photolysis rates become too small to be important due to low absorption cross section for VL. The overall JVL is 7.06E-4 s-1, a few times higher than the kdecay measured (2.3E-4 s-1) and the gas-phase loss rate due to OH reactions (1E-4 s-1). Therefore, we believe that the decay rate due to UV photolysis of VL in the troposphere is at least comparable to that of OH reactions in gas phase. Note that the same UV photolysis can occur in gas phase too.

Figure S14. (a) molar absorption coefficient (from NIST database) and estimated absorption cross section of VL; (b) solar actinic flux in typical tropospheric environments: ground level, July 1, noon, 40°N, 298 K (Finlayson-Pitts and Pitts, 1986) and assumed

quantum yield (0.28) for VL. âĂČ

As mentioned by another commenter, the authors should include information about the pH of reaction solutions in their experiments. Ideally this should be monitored throughout aqueous aging. At a minimum, it should be measured at the beginning and end of each experiment, if not controlled. Please provide pH information and discuss the possible role of varying pH in more realistic atmospheric clouds on the aqueous chemical processing observed here.

R: We agree with the reviewers that pH can be an important parameter on the reactions under study. That is why we measured the H2O2 decay rate in the ammonium sulfate (AS) and ammonium bisulfate (ABS) solutions to first confirm whether the pH affects H2O2 decay or not. As shown in Figure S6, it does not. One can thus investigate the effects of pH on the reactions between organics and OH radical (or direct photolysis). However, as we pointed out in the response to Reviewer #1, too many variables in the experiments might diverge from the current focus of the current manuscript. We plan to investigate the effect of pH on the reactions in future experiments. A discussion on possible pH effects is included in the section of Atmospheric Implications in the revised manuscript, as below.

O: Moreover, the OH radical concentration used was also one order of magnitude higher than typical ambient concentrations.

M: On the other hand, pH in the aqueous droplets will have an effect on the aqueous-phase reactions (Ervens et al., 2011). Commonly found acidic aqueous phase in the atmosphere may not affect the production of OH radical from H2O2 photolysis as shown in Figure S6, where ammonium bisulfate (ABS) was used as the medium for H2O2 UV photolysis at 254 nm, with negligible difference as compared to when AS solution was used as the medium. But the acidic environment may promote hydration of some carbonyl compounds, thus alter the kinetics and even branching ratios of aqueous-phase reactions. In the current study, the pH of the aqueous solution was not controlled, and

a pH value was approximately 6 with 0.1 mM of AS. Further investigation is needed to ascertain the role of acidity in the aqueous-phase reactions of methoxy-phenolic compounds. Moreover, the OH radical concentration used was also one order of magnitude higher than typical ambient concentrations.

Please specify the “dry conditions” RH used in the growth factor experiments and discuss whether the tested particle types are likely to be completely free of water at that RH.

R: the “dry condition” refers to RH < 5% in the first DMA. For ammonium sulfate (AS) particles, crystallization is expected to occur at around RH=30%. Thus, it can be considered to be completely free of water for AS under this dry condition. For AS/organics mixed particles, however, small amounts of water might be retained even at RH < 5%. Using E-AIM II (Clegg et al., 1998), we show below that if the AS particles are mixed with 50% (by molar number) of oxalic acid, the most commonly found hygroscopic dicarboxylic acid in aerosols and surrogate of small oxygenates under condition (A) in this study, would retain a small amount of water even at RH = 5%. This estimation is uncertain because of the high concentrations of the electrolytes and the assumption that the organic portion comprises of oxalic acid only. Nevertheless, this small amount of water will cause only little difference in growth factor measurements and will not affect the conclusion of the current study.

In Case I, aqueous-phase water (H2O(aq)) is only 1.6% by mass of the condensed phase and 2.7% by volume. Translated to diameters, this little amount of water would cause <1% of difference compared to completely dry solid particles.

In case II, aqueous-phase water (H2O(aq)) is 3.5% by mass of the condensed phase and 5.9% by volume. Translated to diameters, this little amount of water would cause <2% of difference compared to completely dry solid particles.

A discussion on this has been added to Section 2.5 in the revised manuscript.

O: The hygroscopic growth factor, GF90, defined as the ratio of the humidified (at 90% RH) particle diameter to the dry particle diameter, was then obtained.

M: The hygroscopic growth factor, GF90, defined as the ratio of the humidified (at 90% RH) particle diameter to the dry particle diameter, was then obtained. Note that under condition (A) when substantial amounts of small oxygenates were formed, the dried particles may not be completely water free. Although there is uncertainty in the estimation without the exact knowledge of the amounts of all the small oxygenates and high electrolyte concentrations, EIM-II (Clegg et al., 1998) predicted a <2% difference in the Ddry.

“bond” should be changed to “bound” in line 14 of the supplement

R: changed as suggested.

“maker” should be changed to “marker” in line 4 of p. 27644

R: changed as suggested.

I prefer the use of the term “saturation vapor pressure” to “saturated vapor pressure,” but that may simply reflect a difference in British vs. American English

R: changed as suggested.

Change “form” to “formed” on line 17 of p. 27646

R: changed as suggested.

Reference Clegg, S. L., Brimblecombe, P., and Wexler, A. S.: Thermodynamic model of the system H+-NH4+-SO42–NO3–H2O at tropospheric temperatures, J. Phys. Chem. A, 102, 2137-2154, 1998. Coeur-Tourneur, C. c., Cassez, A., and Wenger, J. C.: Rate Coefficients for the Gas-Phase Reaction of Hydroxyl Radicals with 2-Methoxyphenol (Guaiacol) and Related Compounds, J. Phys. Chem. A, 114, 11645-11650, 2010. Ervens, B., Turpin, B. J., and Weber, R. J.: Secondary organic aerosol formation in cloud droplets and aqueous particles (aqSOA): a review of

laboratory, field and model studies, Atmos. Chem. Phys., 11, 11069-11102, 2011. Ervens, B., Wang, Y., Eagar, J., Leaitch, W. R., Macdonald, A. M., Valsaraj, K. T., and Herckes, P.: Dissolved organic carbon (DOC) and select aldehydes in cloud and fog water: the role of the aqueous phase in impacting trace gas budgets, Atmos. Chem. Phys., 13, 5117-5135, 2013. Finlayson-Pitts, B. J., and Pitts, J. N. J.: Atmospheric Chemistry: Fundamentals and Experimental Techniques, Wiley, New York, 1986. Li, Y. J., Chen, Q., Guzman, M. I., Chan, C. K., and Martin, S. T.: Second-generation products contribute substantially to the particle-phase organic material produced by beta-caryophyllene ozonolysis, Atmos. Chem. Phys., 11, 121-132, 2011. Seinfeld, J. H., and Pandis, S. N.: Atmospheric chemistry and physics: From air pollution to climate change, 2nd ed., Wiley, New Jersey, 2006. Sun, Y. L., Zhang, Q., Anastasio, C., and Sun, J.: Insights into secondary organic aerosol formed via aqueous-phase reactions of phenolic compounds based on high resolution mass spectrometry, Atmos. Chem. Phys., 10, 4809-4822, 2010. Talrose, V., Stern, E. B., Goncharova, A. A., Messineva, N. A., Trusova, N. V., and Efimkina, M. V.: NIST Standard Reference Database 69: NIST Chemistry WebBook, in, 2007.

Please also note the supplement to this comment:
http://www.atmos-chem-phys-discuss.net/13/C11218/2014/acpd-13-C11218-2014-supplement.pdf

---

Interactive comment on Atmos. Chem. Phys. Discuss., 13, 27641, 2013.

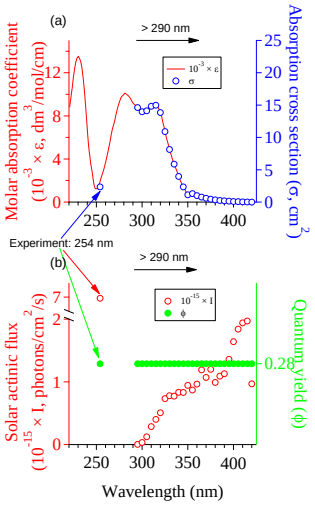

Fig. 1.

Table S4. Estimation of wavelength-dependent photolysis rates of VL.

Wavelength λ (nm)	$\bar{I}$ (photons cm^{-2} s^{-1})	$10^{20} \times \sigma_{VL}$ (cm^2)	ϕ_{VL}	J_{VL} (s^{-1})
254 (condition B)	**6.92×10^{15}**	**2.35**	**0.28**	**2.3×10^{-4}**
295-300	3.14×10^{12}	15	0.28	6.42×10^{-7}
300-305	3.35×10^{13}	14	0.28	6.56×10^{-6}
305-310	1.24×10^{14}	14	0.28	2.45×10^{-5}
310-315	2.87×10^{14}	15	0.28	5.96×10^{-5}
315-320	4.02×10^{14}	15	0.28	8.43×10^{-5}
320-325	5.08×10^{14}	14	0.28	9.85×10^{-5}
325-330	7.34×10^{14}	11	0.28	1.12×10^{-4}
330-335	7.79×10^{14}	8.1	0.28	8.88×10^{-5}
335-340	7.72×10^{14}	5.9	0.28	6.34×10^{-5}
340-345	8.33×10^{14}	4	0.28	4.63×10^{-5}
345-350	8.32×10^{14}	2.4	0.28	2.74×10^{-5}
350-355	9.45×10^{14}	1.1	0.28	1.49×10^{-5}
355-360	8.71×10^{14}	1.3	0.28	1.59×10^{-5}
360-365	9.65×10^{14}	1	0.28	1.36×10^{-5}
365-370	1.19×10^{15}	0.78	0.28	1.30×10^{-5}
370-375	1.07×10^{15}	0.6	0.28	8.95×10^{-6}
375-380	1.20×10^{15}	0.46	0.28	7.67×10^{-6}
380-385	9.91×10^{14}	0.35	0.28	4.81×10^{-6}
385-390	1.09×10^{15}	0.26	0.28	3.97×10^{-6}
390-395	1.13×10^{15}	0.19	0.28	3.05×10^{-6}
395-400	1.36×10^{15}	0.14	0.28	2.66×10^{-6}
400-405	1.64×10^{15}	0.099	0.28	2.26×10^{-6}
405-410	1.84×10^{15}	0.066	0.28	1.71×10^{-6}
410-415	1.94×10^{15}	0.041	0.28	1.11×10^{-6}
415-420	1.97×10^{15}	0.021	0.28	5.85×10^{-7}
420-425	9.69×10^{14}	0.0057	0.28	7.78×10^{-8}
	Total (295-425 nm)			**7.06×10^{-4}**

Fig. 2.

Table R1 E-AIM II inputs:

	Case I (solid formation allowed)	Case II (solid formation not allowed)
Temperature (K)	298.15	
Relative humidity (%)	5	
Ammonium sulfate (mole)	1E-6	
Oxalic acid (mole)	1E-6	
Solid formation	$(NH_4)_2SO_4$, $HOOCCOOH{\cdot}2H_2O$	-

E-AIM II outputs:

Table R2. Output from E-AIM II with Cases I and II.

Species	Mass (gram)	
	Case I	Case II
H(aq)	4.80E-10	1.18E-10
NH4(aq)	4.07E-07	3.61E-05
HSO4(aq)	4.99E-07	3.30E-05
SO4(aq)	5.91E-07	6.34E-05
OH(aq)	2.73E-24	1.60E-28
HOxal-(aq)	4.92E-07	2.42E-05
Oxal2-(aq)	4.13E-09	2.99E-06
H2O(aq)	1.49E-06	7.99E-06
NH3(aq)	1.43E-16	1.08E-14
Oxalic(aq)	8.95E-05	6.25E-05
H2O(aq) m%[1]	1.59	3.47
H2O(aq) v%[2]	2.71	5.90
Diameter increase (%)[3]	0.9	1.9

Note [1]mass percentage of liquid water; [2] assuming AS and oxalic acid dihydrate have a similar density of 1700 kg/m^3 (1770 for AS and 1650 for oxalic acid dehydrate) and liquid water density of 1000 kg/m^3; [3]compared to completely dried particles.

Fig. 3.